

Comparative study of the seismic response of RC framed buildings retrofitted using modern techniques

Fabio Mazza*

Dipartimento di Ingegneria Civile, Università della Calabria, 87036 Rende (Cosenza), Italy

(Received November 25, 2014, Revised March 21, 2015, Accepted April 7, 2015)

Abstract. The main purpose of this work is to compare different criteria for the seismic strengthening of RC framed buildings in order to find the optimal combinations of these retrofitting techniques. To this end, a numerical investigation is carried out with reference to the town hall of Spilinga (Italy), an RC framed structure with an L-shaped plan built at the beginning of the 1960s. Five structures are considered, derived from the first by incorporating: carbon fibre reinforced polymer (FRP)-wrapping of all columns; base-isolation, with high-damping-laminated-rubber bearings (HDLRBs); added damping, with hysteretic damped braces (HYDBs); FRP-wrapping of the first storey columns combined with base-isolation or added damping. A three-dimensional fibre model of the primary and retrofitted structures is considered; bilinear and trilinear laws idealize, respectively, the behaviour of the HYDB, providing that the buckling be prevented, and the FRP-wrapping, without resistance in compression, while the response of the HDLRB is simulated by using a viscoelastic linear model. The effectiveness of the retrofitting solutions is tested with nonlinear dynamic analyses based on biaxial accelerograms, whose response spectra match those in the Italian seismic code.

Keywords: seismic retrofit of framed buildings; fibre-reinforced-polymer structure; base-isolated structure; added-damping structure; nonlinear dynamic analysis

1. Introduction

The seismic retrofitting of existing structures, in particular of RC buildings designed for vertical loads only or with inadequate seismic classifications and seismic code provisions, represents a far-reaching problem requiring urgent action. Traditional methods, usually adopting conventional materials and construction techniques, can be classified into two conceptual categories (Oliveto and Marletta 2005, Thermou and Elnashai 2006): one based on increasing strength and stiffness, by adding new structural elements to the system (e.g., RC shear wall or steel brace) and/or enlarging the existing members (e.g., steel encasing or concrete jacketing), and the other based on mass reduction. Modern methods, based on new techniques and materials, can be schematically subdivided into three categories (Thermou and Elnashai 2006, Calvi 2013): modification of damage and collapse modes of the structure (Di Ludovico *et al.* 2008, Baratta and Corbi 2012), to eliminate possible sources of brittle failures (e.g., by wrapping an element or part

*Corresponding author, Professor, E-mail: fabio.mazza@unical.it

of it, with carbon, glass and aramidic fibre reinforced polymer (FRP)); increasing deformability, at the base of the building, with a considerable reduction of the seismic loads transmitted to the superstructure (Naeim and Kelly 1999); added damping, to reduce the seismic demand rather than increasing the capacity (Christopoulos and Filiatrault 2006, Mazza and Vulcano 2007, Ponzo *et al.* 2012, Sorace and Terenzi 2008, Baratta *et al.* 2012, Tirca *et al.* 2003).

In the present work, the town hall of Spilinga, a small town near Vibo Valentia (Italy), is considered for the numerical investigation. Specifically, an RC framed structure, with an L-shaped plan, was built at the beginning of the 1960s according to the Italian seismic code in force at the time of construction (Royal Decree-Law 1937), for a high-risk seismic region and a medium subsoil class (Royal Decree-Law 1935). Firstly, the seismic vulnerability of the Spilinga building is investigated with reference to serviceability and ultimate limit states provided by the Italian (NTC08 2008) and European (Eurocode 8 2004) seismic codes. Then, for the purpose of retrofitting the primary structure, assuming high-risk seismic region and a soft subsoil class, five alternative structural solutions are examined: (a) the carbon fibre reinforced polymer (FRP) retrofitted structure, with FRP-wrapping of all columns limited to their critical end zones; the base isolation (BI) retrofitted structure, with high-damping-laminated-rubber bearings (HDLRBs); (c) the added damping (AD) retrofitted structure, with hysteretic damped braces (HYDBs) in the exterior spans of the perimeter plane frames; (d) the FRP+BI retrofitted structure, combining wrapping of the first-storey columns and base-isolation; (e) the FRP+AD retrofitted structure, combining wrapping of the first-storey columns and added damping.

Nonlinear dynamic analyses are carried out on a three-dimensional fibre model (SeismoStruct 2010) of the primary and retrofitted structures; bilinear and trilinear laws idealize, respectively, the behaviour of HYDB, providing that buckling be prevented, and FRP, without resistance in compression, while the response of an HDLRB is simulated by using a viscoelastic linear model. Biaxial accelerograms are considered, whose response spectra match those adopted by NTC08 for the seismic design levels corresponding to the serviceability (i.e., full-operational, FO, and operational, OP) and ultimate (i.e., life-safety, LS) limit states. The effectiveness of the retrofitting solutions is examined by checking that under FO and OP ground motions, inter-storey drifts are confined within the capacity thresholds, while under LS ground motions, ductile (at the member level) and brittle (at the section level) mechanisms are not reached.

2. Test structure

The case study selected for this work is the town hall of Spilinga (Fig. 1), a small town near Vibo Valentia (Italy). In particular, an RC framed structure, with an L-shaped irregular plan with storey heights of 3.3 m (1st level) and 2.9 m (2nd level), was built at the beginning of the 1960s. The structure was designed to comply with the admissible tension method, according to the Italian seismic code in force at the time of construction (Royal Decree-Law 1937), for a high-risk seismic region (degree of seismicity $S=12$, which corresponds to a coefficient of seismic intensity $C=0.10$) and a medium subsoil class (Royal Decree-Law 1935). The geometric dimensions and direction of the floor slabs are plotted in Fig. 1(b). The gravity loads are represented by dead and live loads, whose values are, respectively, equal to: 5.1 kN/m² and 3 kN/m², on the first floor; 3.9 kN/m² (including also the weight of the roof) and 0.5 kN/m², on the second floor. The contribution of the masonry-infills, made with two layers of full bricks with a thickness of 0.12 m each, is taken into account in the mass and stiffness distribution assuming a weight of 2.7 kN/m² and a modulus of

elasticity of 1500 MPa, respectively. The expression proposed by Mainstone (1974) is considered to evaluate the area of the equivalent diagonal strut. Section dimensions of columns (c), constant along the two storeys, and deep (d) and flat (f) girders are reported in Table 1 according to the typologies of cross-section shown in Fig. 1(c); it is worth noting that some deep girders in Fig. 1(c) had second floor dimensions (see symbols in brackets) which were greater than those on the first floor. In Fig. 1(d) labels of columns (i.e., $i_c, i=1,20$) and girders (i.e., $i_g, i=1,29$) are reported to identify the structural elements at each storey. Finally, RC dog-legged stairs are also plotted in Fig. 1(b), with four columns (i.e., $9_c, 10_c, 13_c$ and 14_c columns shown in Fig. 1(d)) delimiting a rectangular area of about $2.80 \text{ m} \times 3.75 \text{ m}$.

A total mass of the building equal to 458 ton, subdivided between 268 ton and 190 ton on the first and second floor, respectively, is assumed. In Table 2, the following dynamic properties are reported for the two translational modes along the main axes in plan (i.e., X and Y axes in Fig. 2) and the torsional mode around the vertical axis (i.e., Z axis): the vibration period (T); the effective modal masses in the X (i.e., $m_{E,X}$) and Y (i.e., $m_{E,Y}$) directions, expressed as percentages of the total mass (m_t) of the structure. Moreover, the position of the mass centres, on the first (i.e., $C_{M,1}$) and

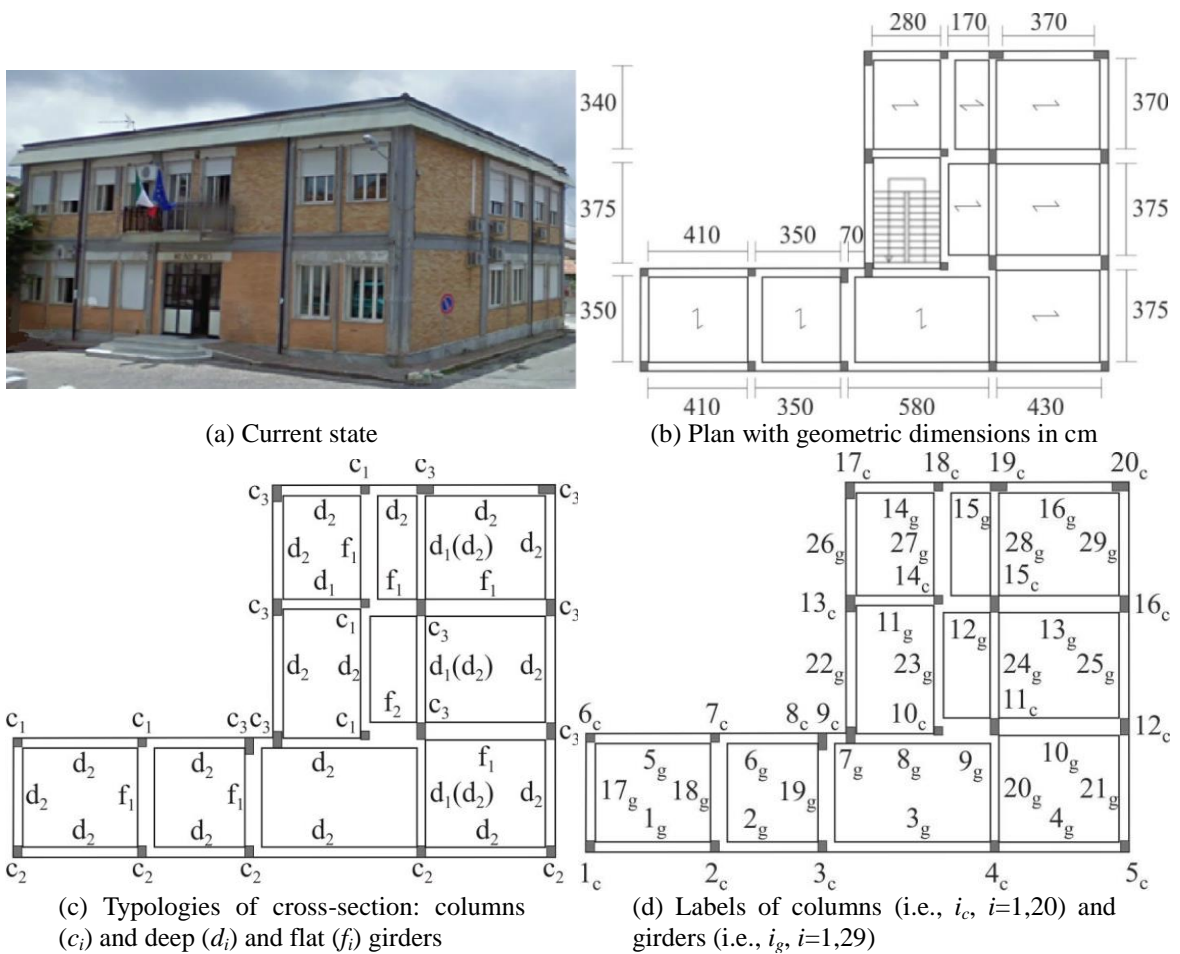


Fig. 1 Town hall of Spilinga (Vibo Valentia, Italy)

Table 1 Section dimensions (in cm) of columns (*c*) and deep (*d*) and flat (*f*) girders

Type	c_1	c_2	c_3	d_1	d_2	f_1	f_2
	30×30	30×40	30×60	30×40	35×50	60×21	90×21

Table 2 Dynamic properties of the test structure

Vibration mode	T (s)	$m_{E,X}$ (% m_t)	$m_{E,Y}$ (% m_t)
1	0.42	73.9	3.5
2	0.30	3.5	36.9
3	0.35	15.2	49.8

$$*m_t = m_1 + m_2 = 268 + 190 = 458 \text{ ton}$$

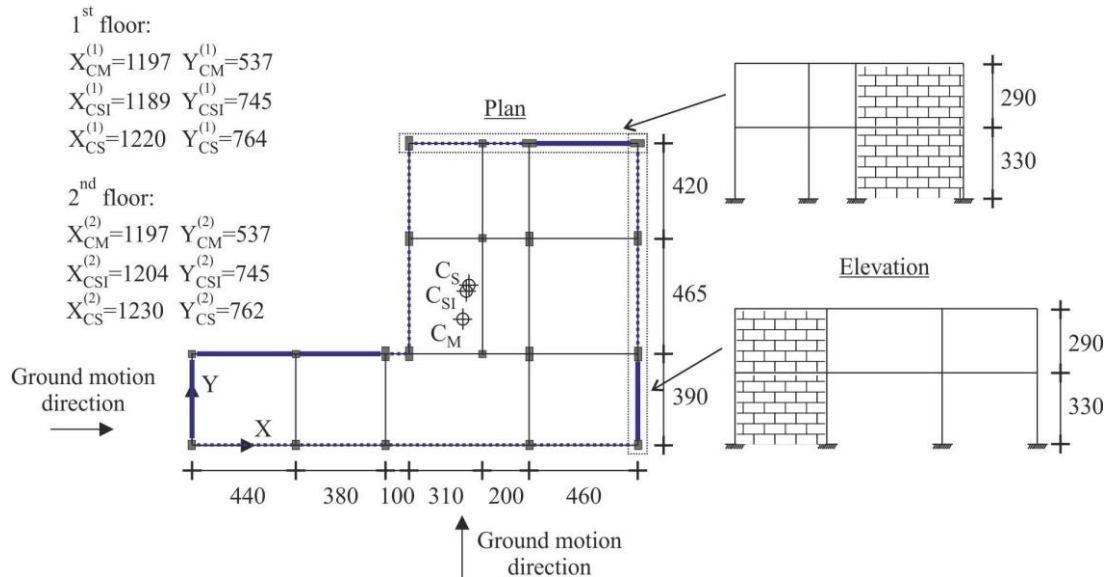


Fig. 2 Plan and elevation of the Spilinga building (dimensions in cm)

second (i.e., $C_{M,2}$) floor, and the analogous stiffness centres, where the infills are considered (i.e., $C_{SI,1}$ and $C_{SI,2}$, at the full-operational, FO, and operational, OP, limit states) or neglected (i.e., $C_{S,1}$ and $C_{S,2}$, at the life-safety, LS, limit state), are plotted in Fig. 2. In detail, the in-plan distribution of masonry infills is shown in Fig. 2, where only the infills placed in the bays without openings and highlighted in plan with a solid blue line are considered in the evaluation of the stiffness centres.

In 2004, the Administration of Spilinga carried out an investigation of the building, including a geometric survey and the characterization of the structure by means of material controls. Concrete properties were investigated by means of direct (i.e., core testing) and indirect tests (i.e., sclerometric and ultra-sonic tests) which allowed the definition of a concrete cylindrical strength equal to 16.6 MPa. Steel properties were estimated according to the Italian standards in force at the time of construction (Royal Decree-Law 1939); since the Aq60 steel was used, a yield strength of 310 MPa was assumed. To improve the knowledge level of the Spilinga building the present work uses a simulated design (Mazza 2014), with reference to the Royal Decree-Law in 1937 and to the seismic classification in 1935 and material properties in 1939 available at the time of construction.

The strengths of concrete and steel have been divided by a confidence factor equal to 1.2 corresponding to a normal level of knowledge, according to NTC08.

2.1 Retrofit with FRP-wrapping of the columns: the FRP retrofitted structure

FRP-wrapping of columns is one of the most effective seismic retrofitting techniques of RC framed structures. As confirmed by experimental (e.g., Balsamo *et al.* 2005) and numerical (e.g., Ferracuti *et al.* 2006) results, it enables the development of large chord rotation ductility factors and avoids the activation of brittle failure modes. An appropriate strength hierarchy at both local (i.e., upgrade of single elements) and/or global (i.e., achievement of an assigned global mechanism) can be ensured by selecting the type of fibers and their orientation and evaluating thickness (t_f), width (b_f) and number of layers (n_f) of FRP. For the purpose of retrofitting the performance levels of the Spilinga building in line with the provisions imposed by NTC08, assuming soft subsoil class (subsoil type D) for the geographical coordinates (longitude 15.91° and latitude 38.63°) at the site where the town hall is located, carbon fibre reinforced polymer (FRP) wrapping of the critical (end) zones of all the columns, without modifying the position of the centre of stiffness (C_S) of the primary structure at each storey (Fig. 3), is considered.

The design of the FRP has been carried out according to the provisions of CNR-DT 200 (2004). Specifically, the confinement of an RC frame member, which aims both at increasing the ultimate strength and the ductility, depends only on a fraction of the confinement pressure (f_l). The effective confinement lateral pressure exerted by the FRP, function of member cross-section and FRP configuration, can be expressed as

$$f_{l,eff} = k_{eff} \cdot f_l \geq 0.05 f_{cd} \quad (1)$$

where f_{cd} is the design strength of the unconfined concrete, while k_{eff} represents a coefficient of efficiency (≤ 1), defined as the ratio between the volume of confined concrete and the total volume

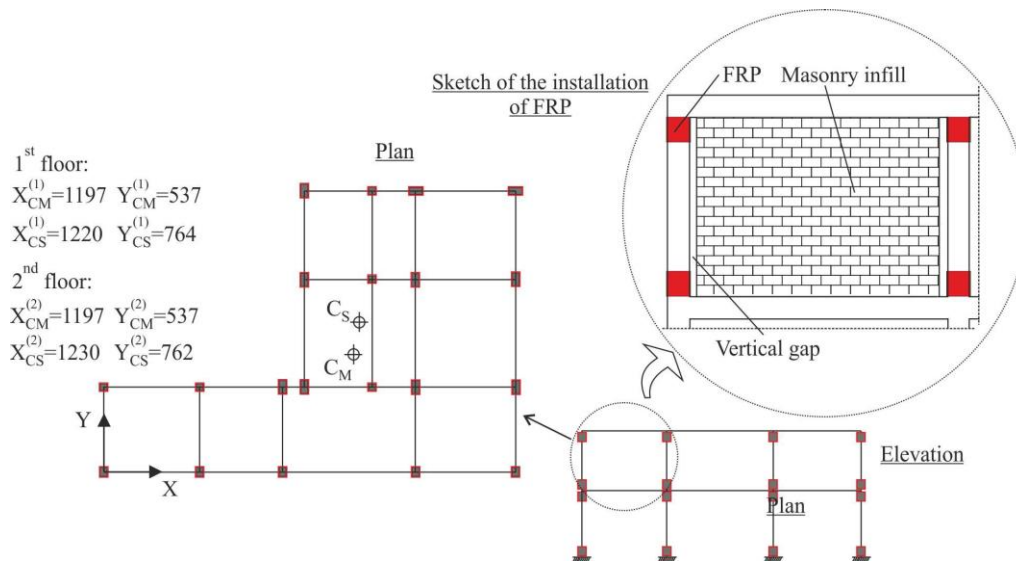


Fig. 3 Plan and elevation of the Spilinga building retrofitted with FRP (dimensions in cm)

of concrete, expressed as product of horizontal (k_H), vertical (k_V) and inclined (k_α) efficiency coefficients

$$k_{eff} = k_H \cdot k_V \cdot k_\alpha \quad (2)$$

The confining pressure can be calculated as

$$f_l = 0.5 \cdot \rho_f \cdot E_f \cdot \varepsilon_{fd,rid} \quad (3)$$

where E_f is the modulus of elasticity of the FRP, with a volumetric ratio of FRP confined members ρ_f and an ultimate strain

$$\varepsilon_{fd,rid} = \min \left\{ \eta_a \varepsilon_{fk} / 1.1; 0.004 \right\} \quad (4)$$

$\eta_a (=0.95)$ being a conversion factor related to environmental conditions.

For the case of continuous wrapping of a rectangular section, with dimensions $b \times d$ and corners rounded with a radius $r_{\geq 20}$ mm, the geometrical percentage of reinforcement can be computed by

$$\rho_f = \left[2t_f \cdot n_f \cdot (b+d) \right] / (b \cdot d) \quad (5)$$

while the characteristic rupture strain can be evaluated as

$$\varepsilon_{fk} = f_{fk} / E_f = (\alpha_{ff} \cdot f_{fib}) / (\alpha_{fE} \cdot E_{fib}) \quad (6)$$

considering safety factors for both stiffness, $\alpha_{fE} (=0.9)$, and strength, $\alpha_{ff} (=0.9)$ and assuming $E_{fib} = 230000$ MPa and $f_{fib} = 4800$ MPa. In Fig. 4 details of the FRP-wrapping of the columns labeled in Fig. 1(d) are summarized, according to the procedure described below.

All masonry infill walls are supposed to be isolated from the adjoining frame before the FRP-wrapping of the columns limited to their critical (end) zones. Thus, the infill walls separated from the RC frame do not contribute significantly to the lateral stiffness and strength of the building but their out-of-plane stability needs to be recovered. A sketch of the FRP installation around a column of the original structure is also shown in Fig. 3.

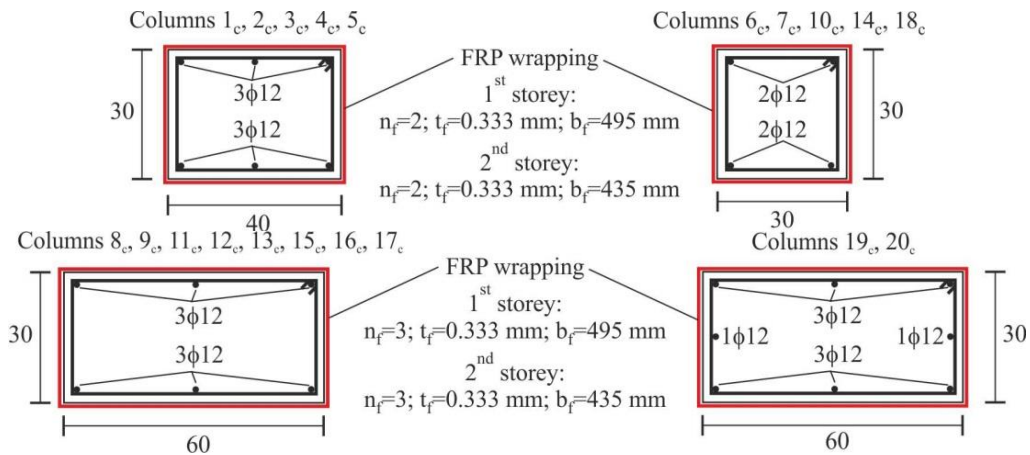


Fig. 4 Geometrical properties of the FRP-wrapping of the columns (dimensions in cm)

2.2 Retrofit with base-isolation: the BI retrofitted structure

Given the limited number of storeys of the Spilinga building it would be possible to uplift the whole structure and to create an independent foundation, in order to insert isolators between the double foundation system. To do this, we assume a total mass of the base-isolated structure equal to 695 ton, subdivided between 458 ton of the superstructure, where masonry infill walls as nonstructural elements are considered, and 237 ton of the foundation above the isolation system, respectively. As shown in Fig. 5, the Spilinga building is supported by twelve identical HDLRBs thereby limiting, at the foundation level (-1), the eccentricity between the stiffness centre of the isolation system (C_S) and the projection of the centre of mass (C_M) of the superstructure.

The proportioning of the HDLRBs has been carried out on the assumption that, besides the gravity loads, the horizontal loads correspond to a behaviour factor $q=1.0$; the acceleration design spectrum is modified in the period range $T \geq 0.8T_s$, assuming an equivalent viscous damping ratio of the isolation system (i.e., ξ_{Is}), at shear deformation $\gamma=1$, equal to 15%. Moreover, the Italian seismic code (NTC08) requires that the fundamental vibration period of the base-isolated structure (i.e., T_{Is}) be in the range $3T_{BF} \leq T_{Is} \leq 3s$, T_{BF} being the fundamental vibration period of the same structure on fixed-base (see Table 2). In the present case a reasonable isolation period was $T_{Is}=1.8s$.

The HDLRBs fulfill the ultimate limit state verifications regarding the maximum shear strains: i.e., $\gamma_{tot} = \gamma_s + \gamma_c + \gamma_\alpha \leq 5$ and $\gamma_s \leq 2$, where γ_{tot} represents the total design shear strain, while γ_s , γ_c and γ_α represent the shear strains of the elastomer due to seismic displacement, axial compression and angular rotation, respectively. Moreover, the maximum compression axial load (P) did not exceed the critical load divided by a safety coefficient equal to 2.0. The critical buckling load is evaluated as a function of the primary S_1 (e.g., $S_1 \geq 12$ is a conservative assumption to reduce the vertical

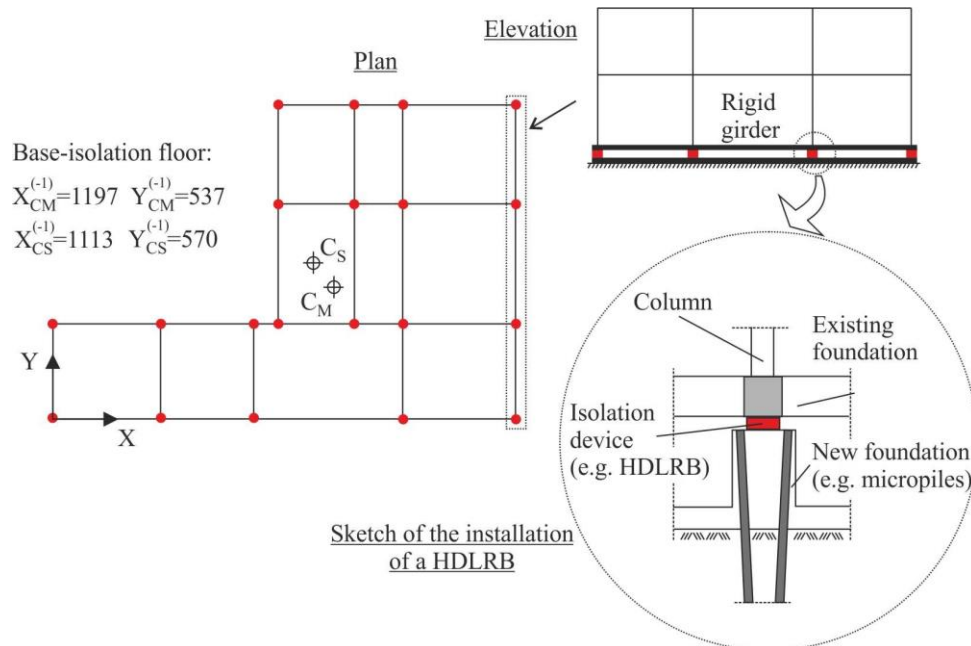


Fig. 5 Plan and elevation of the Spilinga building retrofitted with base-isolation (dimensions in cm)

Table 4 Geometrical and mechanical properties of the HDLRBs

T_{Is} (s)	ξ_{Is} (%)	α_{K0}	G (MPa)	E_b (MPa)	K_{H0} (kN/mm)	K_{V0} (kN/mm)	D (mm)	t_i (mm)	n_i	t_s (mm)	d_{dc} (mm)
1.8	15%	800	0.4	2000	0.423	338	400	8	14	2	230

Table 5 Results of the verifications for the HDRBs

S_1	S_2	γ_s	$\gamma_{tot,max}$	P_{cr}/P_{max}
13	3.4	2	4.98	2

deformability) and secondary S_2 (e.g., $S_2 \geq 4$ is a conservative assumption against buckling) shape factors of the HDLRBs (Mazza and Vulcano 2012, Mazza *et al.* 2012). The minimum tensile stress (σ_t) resulting from the seismic analysis was assumed as $2G$ ($=0.8$ MPa, for a shear modulus of the elastomer $G=0.4$ MPa). Finally, a nominal stiffness ratio α_{K0} , defined as the ratio between the nominal value of the vertical stiffness (K_{V0}) and the analogous value of the horizontal stiffness (K_{H0}), equal to 800 is assumed for the isolators, considering a volumetric compression modulus of the rubber (i.e., E_b) equal to 2000 MPa.

The design of the HDLRBs was carried out according to the steps described in a previous work (Mazza and Vulcano 2011). In Table 4 the following geometrical and mechanical properties are reported: diameter of the bearing (D); thickness of a single elastomeric layer (t_i); number of elastomeric layers (n_i); thickness of a single steel shim (t_s), with a yield strength of 255 MPa; displacement at the collapse prevention limit state (d_{dc}). In Table 5 the results of the ultimate limit state verifications for the HDLRBs are reported. It is worth noting that the design of the isolators depends on the conditions imposed on the maximum values of γ_{tot} and γ_s and the buckling control; no tensile forces were found in the isolators. A sketch of the installation of a HDLRB isolator below a column of the original structure is also shown in Fig. 5. Given the limited number of storeys of the Spilinga building it would be possible to uplift the whole structure and to create an independent foundation, in order to insert isolators between the double foundation system.

2.3 Retrofit with added damping: the AD retrofitted structure

A less expensive solution, in comparison with other retrofitting techniques such as base-isolation, at least in cases of low-rise buildings, is added damping. Hence, the third solution considered in this work involves inserting diagonal steel braces equipped with metallic yielding hysteretic dampers (HYDs) into the Spilinga building. HYDs are independent of temperature and velocity of motion and are generally manufactured from traditional materials and require little maintenance, hence a reliable low cost solution for energy dissipation (e.g., see Christopoulos and Filiatrault 2006). Their behaviour can be idealized by a bilinear law with elastic lateral stiffness K_D and yield force N_y . As shown in Fig. 6, hysteretic damped braces (HYDBs) are placed along the in-plan principal directions, on both storeys, in the external spans of the perimeter plane frames only. The installation modality and in-plan and in-elevation distribution of HYDBs are a relevant matter because geometric restraints usually influence their positioning (e.g., this happens in case of doors, windows, passages and infills). In the present work, HYDBs are placed only in the bays of the perimeter frames without openings (see Fig. 2), supposing that they are inserted between thin precast panels, substituting the existing masonry-infills, which do not contribute significantly to

the lateral stiffness and strength of the building.

New seismic codes only implicitly allow for the use of these devices (e.g., European code, EC8; Italian code, NTC08), while very few codes in the world provide simplified design criteria (e.g., USA code, FEMA 356). In the present work, a DBD procedure the aim of which is to proportion HYDBs for a designated performance level of an existing framed structure, for a specific level of seismic intensity, is considered (Mazza and Vulcano 2008a, b, 2013, 2014a, b). The main steps of the proposed DBD design method are summarized in Fig. 7, where an iterative procedure solves steps 3-5. Specifically, to avoid brittleness, a design value of the frame ductility $\mu_F=1.5(=1.0*\gamma_{LS}$, where e.g., $\gamma_{LS}=1.5$) is considered at the life-safety (LS) limit state; moreover, a design value of the damper ductility $\mu_D=10$ and a hardening ratio $r_D=5\%$ are assumed.

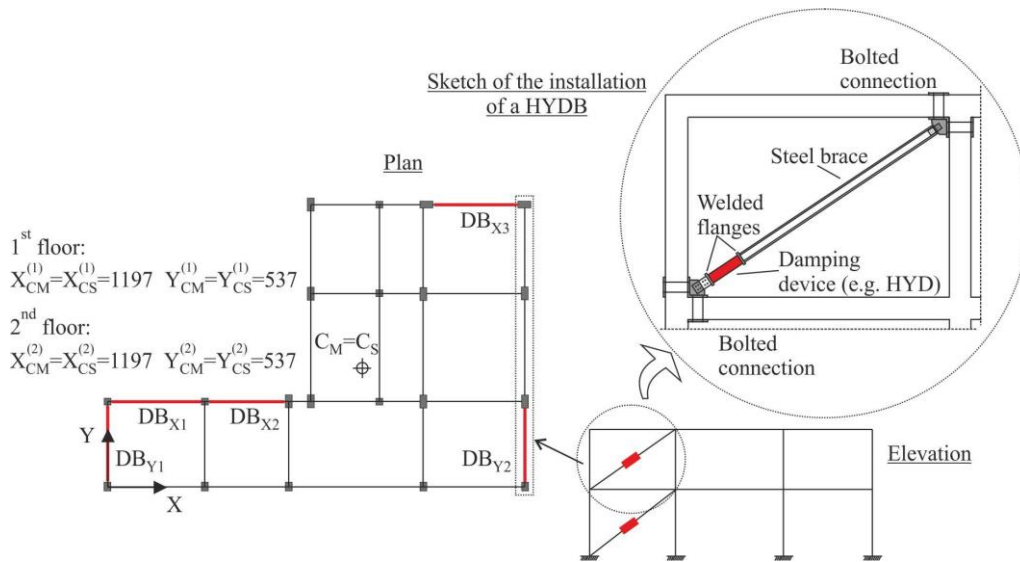


Fig. 6 Plan and elevation of the Spilinga building retrofitted with added damping (dimensions in cm)

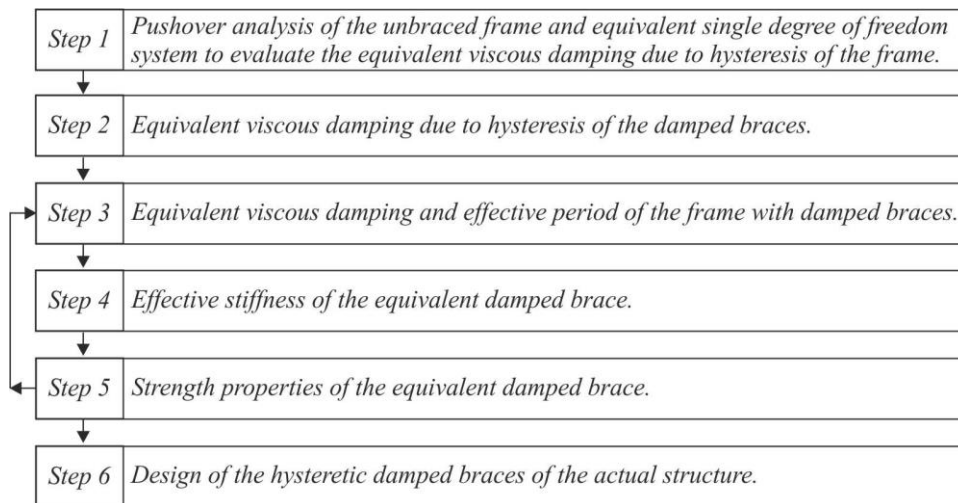


Fig. 7 Flow-chart of the design procedure of the HYDBs

Table 6 Stiffness and strength properties of the HYDBs

Storey	$K_i^{(DB)}$ (kN/m)					$V_{yi}^{(DB)}$ (kN)				
	DB_{x1}	DB_{x2}	DB_{x3}	DB_{y1}	DB_{y2}	DB_{x1}	DB_{x2}	DB_{x3}	DB_{y1}	DB_{y2}
2	82910	93884	13669	200929	128963	214	214	31	281	178
1	101106	117094	74586	317050	190071	305	305	194	504	300

The lateral stiffness of the damped brace (K_{DB}) is assumed equal to the lateral stiffness of the damper (K_D), on the assumption that the brace is much stiffer than the damper it supports (i.e., $K_B \rightarrow \infty$). A position of C_S (after the insertion of HYDBs) equal to that of C_M is assumed, at each storey, in order to eliminate (elastic) torsional effects of the primary structure corresponding to the position of the stiffness centre evaluated without the contribution of the masonry infills (i.e., $C_{S,1}$ and $C_{S,2}$ shown in Fig. 2). To this end, the effective stiffness of the equivalent damped brace (see step 4 of the design procedure shown in Fig. 7) is distributed in accordance with a stiffness criterion inversely proportional to the distance between C_M and the perimeter frame where each HYDB is placed (Fig. 6). A sketch of the installation of a HYDB in a frame span of the original structure is also shown in Fig. 6.

Strength distribution of the HYDBs is assumed to be proportional to the stiffness distribution. In-plan and in-elevation distribution laws of the lateral stiffness (i.e., $K_i^{(DB)}$) and yield-load (i.e., $N_{yi}^{(DB)}$) are reported in Table 6.

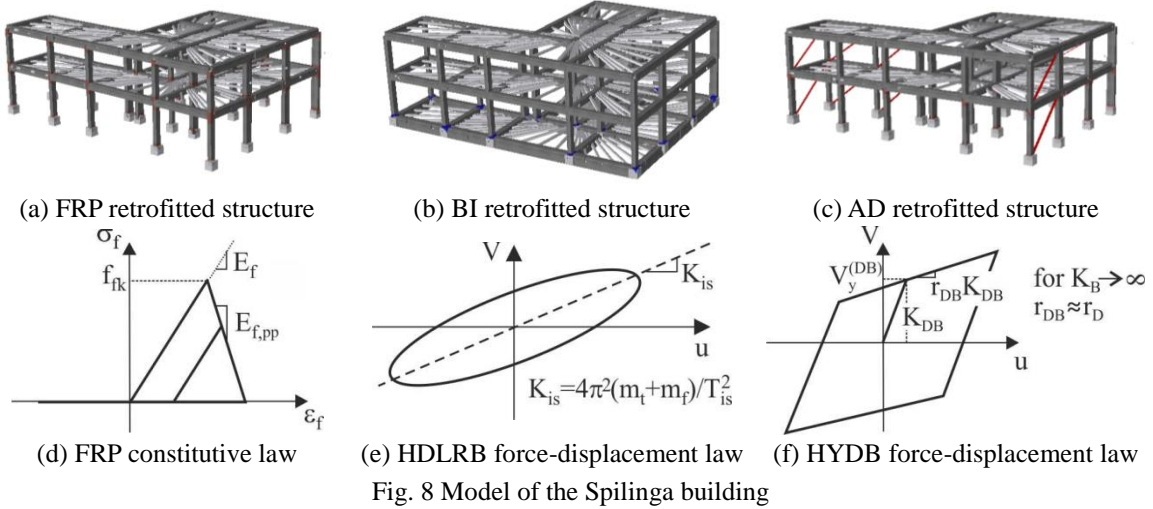
2.4 Retrofit with FRP-wrapping of the columns combined with base-isolation and added damping: the FRP+BI and FRP+AD retrofitted structures

In practice, it is common to find a combination of the strengthening of a selected local element and a global retrofitting, in order to obtain greater seismic performance at lower cost. To this end, carbon FRP-wrapping of the columns, limited to the critical end zones of the first storey, together with base-isolation, with HDLRBs (Fig. 5), or added damping, with HYDBs (Fig. 6), are also considered.

3. Nonlinear modeling and seismic input

In order to study the nonlinear behaviour of the original and retrofitted structures whose properties are illustrated in the previous section, three-dimensional fibre models are considered (SeismoSoft, 2010) in Figs. 8(a)-(c). Force-based fibre elements for girders and columns and special elements for FRP-wrapping of the columns, base-isolation with HDLRBs and added damping with HYDBs are selected. Specifically, each frame member, with length L , is modeled with four sub-elements, two for the critical end zones (with length equal to $0.15L$) and two for the central region (with length equal to $0.35L$). Square and rectangular cross-sections are subdivided into 200 fibres.

The confinement provided by lateral transverse reinforcement is incorporated in the concrete model (Mander *et al.* 1988), to distinguish between unconfined and confined concrete for both critical-end and central regions of each frame member, while the cyclic behaviour of the concrete is also described (Martinez-Rueda and Elnashai 1997). Moreover, the reinforcing steel is modeled



with the Menegotto and Pinto model (1973), coupled with the isotropic hardening rules proposed by Filippou *et al.* (1983) and the buckling rules proposed by Monti and Nuti (1992). The rigid in-plane stiffness of the floor slab is modelled as a rigid diaphragm with elastic truss elements. Bilinear (Fig. 8(f)) and trilinear (Fig. 8(d)) simplified laws idealize, respectively, the behaviour of the HYDB, providing that buckling be prevented, and the FRP, without resistance in compression and with a post-peak modulus $E_{f,pp} = -500000$ MPa, while the response of the HDLRB is simulated by using a viscoelastic linear model (Fig. 8(e)). Finally, masonry infills are represented as equivalent diagonal struts in the primary structure, reacting only in compression at the serviceability limit states with an elastic-brittle linear law. On the other hand, their contribution is neglected in the FRP, BI and AD retrofitted structures.

To evaluate the effects of the proposed retrofitting techniques on the seismic response of the primary structure, nonlinear dynamic analyses were carried out considering biaxial artificial accelerograms applied along the principal directions of the building plan (i.e., X and Y axes in Fig. 2). A set of three artificial motions (labeled as NTC08.D1, NTC08.D2 and NTC08.D3), each with a duration of the stationary part equal to 10 s and a total duration of 25 s, is generated for each limit state prescribed by NTC08 using the computer code SIMQKE (Gasparini and Vanmarcke 1976). Specifically, the elastic response spectra of these motions match (on average) those adopted by NTC08 for the seismic design levels corresponding to the serviceability (i.e., full-operational, FO, and operational, OP) and ultimate (i.e., life-safety, LS) limit states, assuming an elastic viscous damping $\xi_v = 5\%$.

In Fig. 9, taking into account the assumptions made with regard to seismic intensity (i.e., high-risk) and soft subsoil class (i.e., subsoil type D) for retrofitting the primary structure, the following main data are also reported: peak ground acceleration on rock, a_g ; maximum spectrum amplification coefficient, F_0 ; vibration period that marks the start of the constant velocity branch of the design spectrum, T_c^* ; site amplification factor, $S = S_S \cdot S_T$. As shown in Fig. 9, the response spectra of the simulated accelerograms match NTC08 spectrum in the range of vibration periods 0.05 s-2.5 s, which also contains the lower and upper limits of the vibration period prescribed by NTC08 for fixed-base (i.e., $T_{\min} = 0.2T_1$ and $T_{\max} = 2T_1$, where T_1 is the fundamental vibration period of the structure) and base-isolated (i.e., $T_{\min} = 0.2T_1$ and $T_{\max} = 1.2T_1$, where T_1 is the equivalent

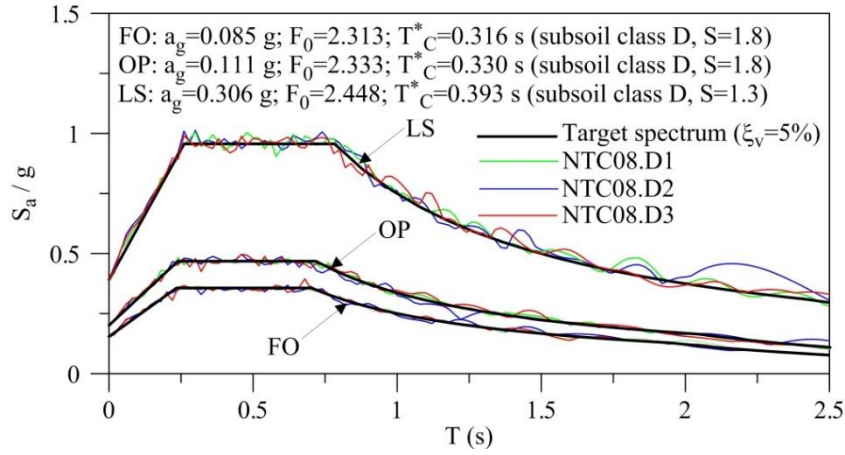


Fig. 9 Acceleration response spectra for full-operational (FO), operational (OP) and life-safety (LS) limit states

vibration period of the isolated structure) structures. This way, the selected accelerograms can be used for the nonlinear dynamic analysis of fixed-base structures with $T_1 \leq 1.25$ s and base-isolated structures with $T_1 \leq 2.1$ s (Iervolino *et al.* 2008).

4. Nonlinear modeling and seismic input

As fully explained below, the capacities of the primary structure in terms of ductile (i.e., chord rotation of columns) and brittle (i.e., shear strength of columns and girders) mechanisms do not satisfy the life-safety (LS) levels evaluated in accordance with NTC08 and EC8 code provisions, respectively. Moreover, the primary structure exceeds the deformability thresholds imposed by NTC08 at the serviceability (i.e., full-operational, FO, and operational, OP) limit states. In the present work, suggestions regarding the effectiveness of FRP-wrapping, base-isolation and added-damping techniques, to control the seismic response at the serviceability and ultimate limit states, and the possible benefits of combining these structural solutions, are provided. To this end, a numerical investigation is carried out to compare the nonlinear dynamic response of the Spilinga building and the retrofitted structures, derived from this by inserting FRPs and/or HDLRBs and HYDBs (i.e., the FRP, BI, AD, FRP+BI and FRP+AD structures shown in Figs. 3-6), subjected to artificially generated biaxial accelerograms.

The effectiveness of the retrofitting solutions is examined by checking that under FO and OP ground motions, inter-storey drifts are confined within capacity thresholds, while under LS ground motions, ductile and brittle mechanisms, with and without axial force, are not reached. The bi-directionality of the horizontal seismic loads and the in-plan irregularity of the structural configuration induce bi-directional inter-storey drift, ductility demand and shear force. For this reason, in order to define serviceability and ultimate limit states (*ls*), the following threshold curve is considered (Mpampatsikos *et al.* 2008)

$$\left(\bar{\beta}_{ls}^{(X)}\right)^2 + \left(\bar{\beta}_{ls}^{(Y)}\right)^2 = 1 \quad , \quad \bar{\beta}_{ls}^{(j)} = \beta_D^{(j)} / \left(\beta_C^{(j)}\right)_{ls} \quad , \quad j \in (X, Y) \quad (7)$$

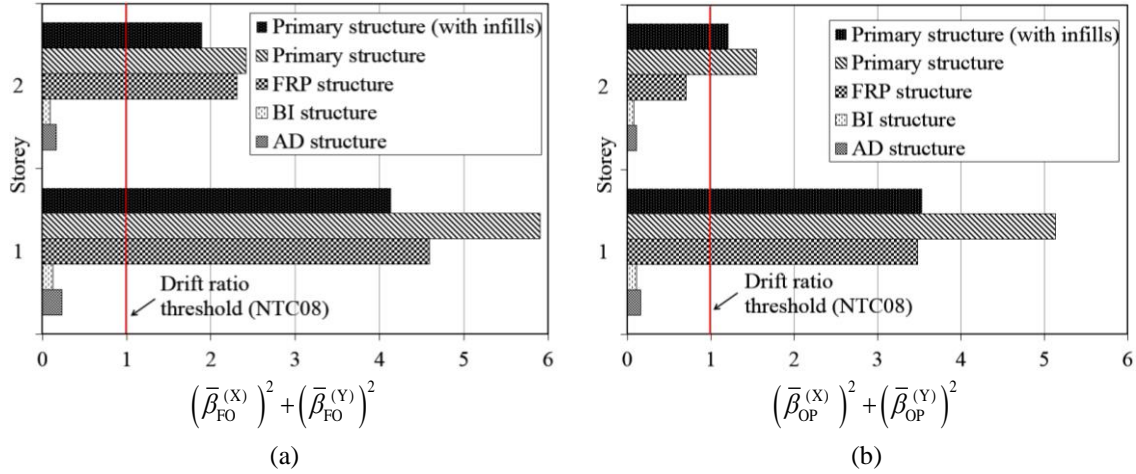


Fig. 10 Dimensionless drift ratio (FO and OP serviceability limit states)

where the l_s demand ($\beta_D^{(j)}$) in the two principal directions (i.e., X and Y axes) is normalized to the corresponding capacity under uniaxial bending ($\beta_C^{(j)}$).

According to the Italian technical regulations (NTC08 2008) accept that FO and OP limit states are reached when the maximum value of the inter-storey drift demand (Δ_{max}) is equal to the capacity (β_C), expressed as a percentage of the storey height (h)

$$\beta_D^{(j)} = \Delta_{max}^{(j)} \quad , \quad (\beta_C^{(j)})_{FO} = 0.33\% h \quad , \quad (\beta_C^{(j)})_{OP} = 0.5\% h \quad , \quad j \in (X, Y) \quad (8)$$

First, the seismic behaviour of the primary and retrofitted (i.e., FRP, BI and AD) structures at the serviceability limit states are examined, checking the deformability thresholds imposed by NTC08 (see Eq. (8)). To this end, maximum values of the dimensionless drift ratio induced by the FO (Fig. 10(a)) and OP (Fig. 10(b)) biaxial ground motions are plotted along the building height, taking into account the definition of the bi-dimensional limit curve (see Eq. (7)). As can be observed, the primary structures, with and without stiffness contribution of the infills, and the FRP-retrofitted structure exceed, at both storeys, the NTC8 deformability thresholds represented by a red line. On the other hand, the BI retrofitted structure proved to be able to control the deformability of the superstructure, provided that the necessary gap at the level of the isolation system is created. Finally, the AD structure is shown to be effective in avoiding a high drift ratio, despite the HYDs having been designed at the LS limit state to avoid their yielding under service gravity loads and moderate seismic loads; thus the AD structure behaves as a braced framed structure at the serviceability FO and OP limit states.

The LS limit state is reached when a ductile or brittle mechanism is obtained. According to NTC08, the ductile mechanism is reached at the member level when the maximum value of the ductility demand ($\mu_{\theta,max}$) equals to $\frac{3}{4}$ of the capacity ($\mu_{\theta,u}$)

$$\beta_D^{(j)} = \mu_{\theta,max}^{(j)} = \frac{g_{max}^{(j)}}{g_y^{(j)}} \quad , \quad (\beta_C^{(j)})_{LS} = \frac{3}{4} \mu_{\theta,u}^{(j)} = \frac{3}{4} \frac{g_u^{(j)}}{g_y^{(j)}} \quad , \quad j \in (X, Y) \quad (9)$$

where θ_{max} is the chord-rotation demand and θ_y and θ_u are the corresponding yielding and ultimate

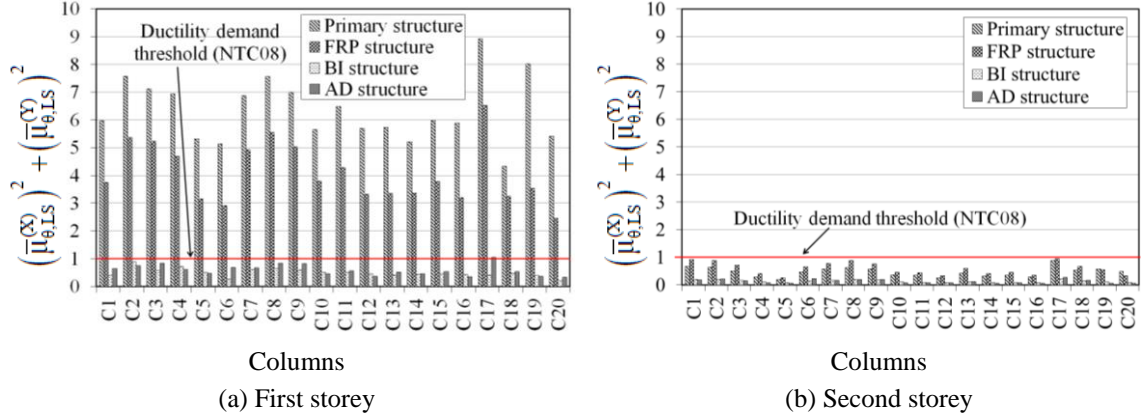


Fig. 11 Dimensionless ductility demand of the columns (LS ultimate limit state)

values. The empirical expression of θ_y and θ_u proposed by EC8 are considered, depending on the material and geometric properties, axial load (P) and shear span (L_s). To simplify the calculation, the axial load due to the gravity loads of the seismic combination (P_V) and a shear span equal to half of the member length ($L_s=L/2$) are considered for all frame members (Mpampatsikos *et al.* 2008, Romão *et al.* 2010).

A similar check is performed for the brittle mechanisms at the section level, through the evaluation of maximum shear demand (V_{max}) and the corresponding capacity (V_u) at the two ends of each structural member

$$\beta_D^{(j)} = V_{max}^{(j)} \quad , \quad \left(\beta_C^{(j)} \right)_{LS} = V_u^{(j)} \quad , \quad j \in (X, Y) \quad (10)$$

According to EC8 (2004), the empirical expression of the shear capacity (V_u) is also assumed as a function of the plastic part of the chord rotation ductility demand.

Afterwards, to check the effectiveness of the FRP, BI and AD retrofitted structures for controlling local damage to the RC columns in the orthogonal principal directions of the building plan (see Eq. (7)), under the LS biaxial ground motions, the maximum values of the dimensionless ductility demand and shear force are shown along the frame height in Figs. 12 and 13, respectively. Preliminarily, the response of the primary structure is examined with reference to the labels shown in Fig. 1(d). In all columns of this structure, ductility demand (see Eq. (9)) and shear force (see Eq. (10)) thresholds are exceeded at the first storey (Figs. 11(a) and 12(a)) but not at the second (Figs. 11(b) and 12(b)). Moreover, the columns undergoing most stress, in terms of ductile and brittle mechanisms, are not generally the same at both storeys.

The FRP retrofitted structure proved to be capable of modifying damage and collapse modes of the primary structure and avoiding brittle failure of the columns (Fig. 12(a)), but it was unable to contain their ductility demand within the NTC08 threshold (Fig. 11(a)). On the other hand, with regard to the control of flexural failure modes of the columns, the reduction of seismic loads transmitted to the superstructure, in the case of HDLRBs, and both the supplementary energy dissipation and limitation of maximum shear force, by inserting HYDs in the diagonal bracings, have made the BI and AD retrofit solutions preferable to FRP (Fig. 11(a)). However, these latter structural solutions are ineffective for controlling the shear force, with a percentage of columns exceeding the EC8 threshold in the first storey equal to 50% and 45% for the BI and AD retrofitted

structures, respectively.

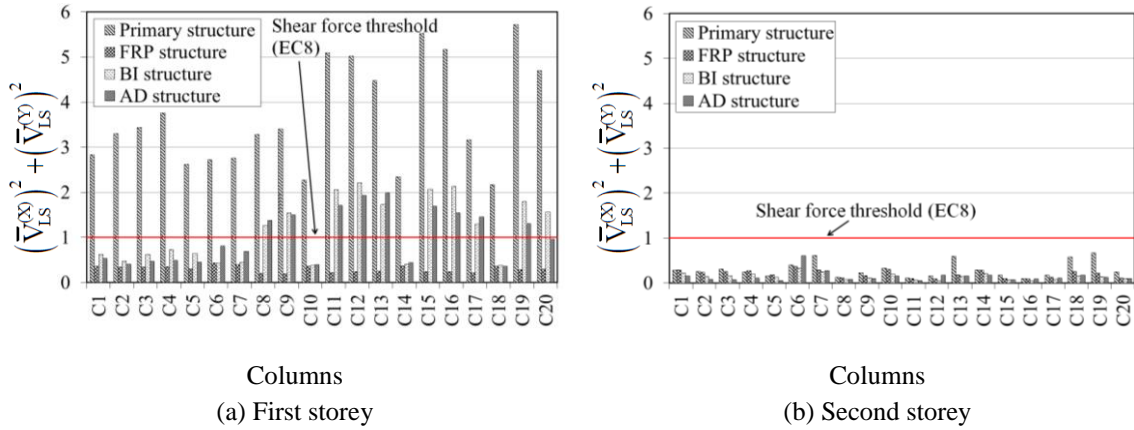


Fig. 12 Dimensionless shear force of the columns (LS ultimate limit state)

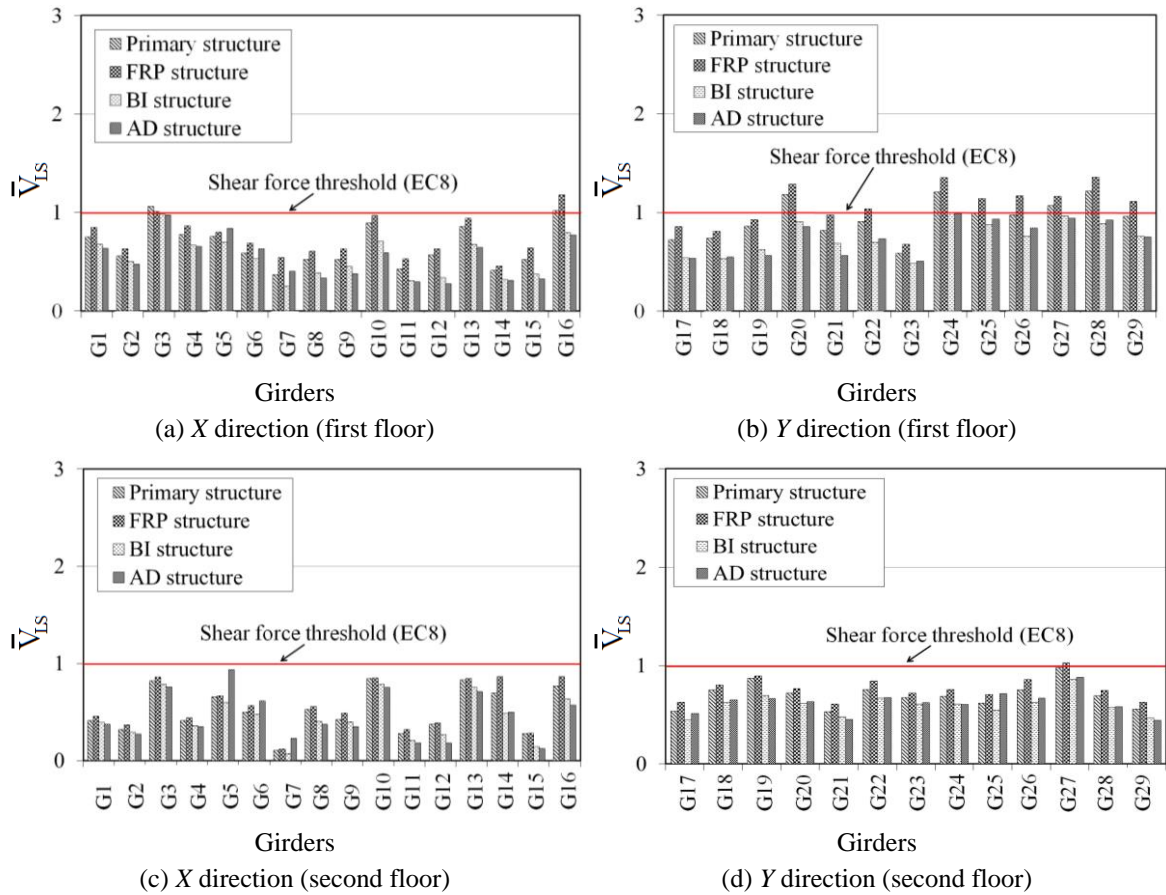


Fig. 13 Dimensionless shear force of the girders (LS ultimate limit state)

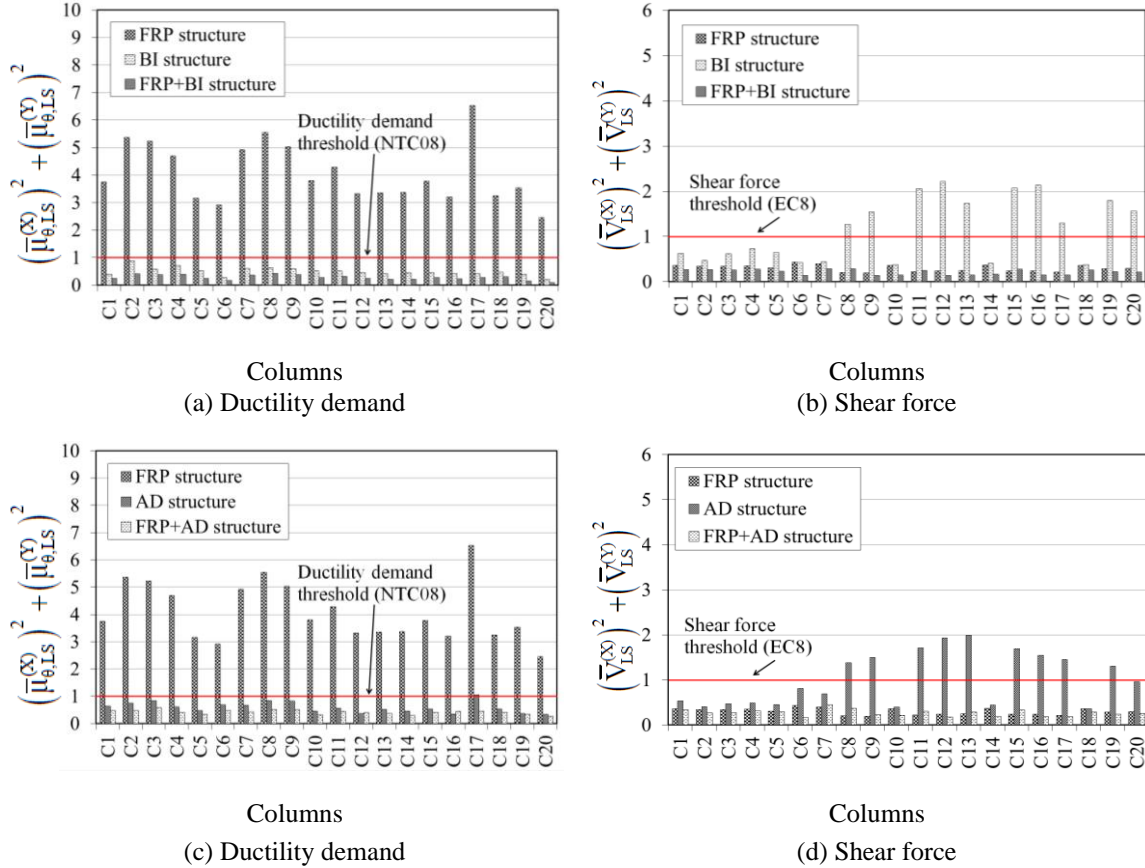


Fig. 14 Dimensionless parameters for the columns of the first storey

In Fig. 13 histograms analogous to those shown above are reported with reference to the dimensionless uniaxial shear force of the RC girders labelled as in Fig. 1(d), on the first (Figs. 13(a), (b)) and second (Figs. 13(c), (d)) floors. In this case, about 21% of the girders on the first floor of the primary structure have exceeded the EC8 shear force threshold highlighted with a red line, especially in the Y direction of the building plan (Fig. 13(b)). As can be observed, an overall increase in shear force is obtained in the case of the FRP retrofitted structure, in comparison with the primary structure, which is unable to furnish an effective solution for about 28% and 4% of the girders on the first (Figs. 13(a), (b)) and second (Figs. 13(c), (d)) floor, respectively. This behaviour can be explained by the fact that increasing the strength of the columns, by FRP wrapping of their critical end zones, leads to a shift of the shear collapse to the girders. As a consequence, failure modes of girders and columns should not be viewed separately, because seismic retrofitting for a deficiency does not necessarily improve overall performance. On the other hand, the results show that the BI and AD retrofitted structures are effective in controlling the shear forces in the girders, which prove to be well within the threshold imposed by EC8. Further results, omitted for the sake of brevity, have indicated that both primary and retrofitted structures satisfy the LS limit state in terms of the ductility demand for girders.

As shown above, seismic retrofitting with modern techniques (i.e., FRPs, HDLRBs and HYDBs), carried out both to limit deformability at the FO and/or OP serviceability limit states and to enhance ductility and/or shear capacity at the LS ultimate limit state, may be insufficient on their own. More specifically, FRP wrapping of the frame members aims to control structural damage but does not address the question of reducing nonstructural damage. On the other hand, ductile and brittle failure modes should be examined at the same time, since: retrofitting of the columns may shift the problem to the girders (e.g., see the FRP retrofitted structure); retrofitting to obtain a flexural strengthening, assuming an elastic response (i.e., $q=1$ in the case of HDLRBs) or limiting the design value of the ductility (i.e., $\mu_r=1.5$ in the case of HYDBs), may shift the problem to a shear failure mode (e.g., see the BI and AD retrofitted structures).

To overcome these problems, it is often advisable to adopt different approaches for a better overall performance. To this end, FRP-wrapping combined with base-isolation and added damping are considered in the present work. Results for the FRP and BI retrofitted structures or the FRP and AD retrofitted structures and their combinations are compared in Figs. 14(a), (b) and 14(c), (d), respectively. In particular, histograms of the maximum values of the dimensionless ductility demand (Figs. 14(a) and 14(c)) and shear force (Figs. 14(b) and 14(d)) in the columns of the first storey, exhibiting problems in the FRP, BI and AD retrofitted structures shown above, are reported. As expected, the FRP+BI and FRP+AD retrofit solutions proved to be, on the whole, satisfactory for seismic protection of the columns at the LS limit state. Moreover, further results, omitted for the sake of brevity, confirmed their effectiveness in satisfying the LS limit state, in terms of girders' shear force, and the FO and OP serviceability limit states, in terms of drift ratio.

5. Conclusions

For the purpose of retrofitting an RC L-shaped framed building, the town hall of Spilinga (Italy), in a high-risk seismic region with a soft subsoil class, fibre reinforced polymer wrapping of the columns, either alone or in combination with base-isolation and added damping is inserted in the primary structure. Even though more case studies are still needed to validate the overall results, the following conclusions can be drawn from the comparison of the nonlinear dynamic biaxial response obtained for the primary structure and those corresponding to five alternative structural solutions (FRP, BI, AD, FRP+BI and FRP+AD retrofitted structures).

At the FO and OP limit states, the primary and FRP retrofitted structures proved to be unsatisfactory for the control of seismic-induced deformability. Both structures satisfy the LS limit state in terms of the ductility demand for girders. The FRP retrofitted structure avoids brittle failure of the columns but it is not capable of containing their ductility demand within the NTC08 threshold. Moreover, the retrofitting of the columns has shifted the problem to the girders where a generalized increase of the shear force is obtained and the EC8 threshold is exceeded at the first floor.

The BI and AD structures are preferable to the FR one for preventing high deformability at the serviceability limit states. With regard to the control of flexural failure modes of the columns, at the ultimate limit state, the BI and AD retrofit solutions ensure that the ductility threshold of NTC08 is not exceeded. However, these structural solutions are ineffective as regards the shear force threshold imposed by EC8 for the columns. Finally, the results show that the BI and AD retrofitted structures are effective in controlling the shear force in the girders, which proved to be well within the EC8 threshold.

As shown above, the seismic retrofitting with FRPs, HDLRBs and HYDBs may be ineffective in controlling some limit states and thus requires a combination of different strengthening approaches. As expected, the FRP+BI and FRP+AD retrofitted structures proved to be satisfactory on the whole for both the control of the FO and OP drift ratios, at the serviceability limit states, and the seismic protection in terms of LS ductility demand and shear force, at the ultimate limit state. Even though the above results were obtained for a single case study, they show the effects which, in general, can be obtained by FRPs and/or HDLRBs or HYDBs, and provide useful suggestions for optimal combinations of these retrofitting techniques. Specifically, the FRP wrapping ensures shear and flexural strengthening and confinement of frame members but ignores the issue of nonstructural damage. Moreover, ductile and brittle failures should be examined together, since: retrofitting of the columns may shift the problem to girders (e.g., the ductility demand of girders for the FRP-retrofitted structure); retrofitting to obtain flexural strengthening may shift the problem to a shear failure mode (e.g., the shear force of columns for the BI and AD retrofitted structures).

Acknowledgments

The present work was financed by Re.L.U.I.S. (Italian network of university laboratories of earthquake engineering), according to “convenzione D.P.C. – Re.L.U.I.S. 2010-2013, task 2.3.2”.

References

- Balsamo, A., Colombo, A., Manfredi, G., Negro, P. and Prota, A. (2005), “Seismic behaviour of a full-scale RC frame repaired using CFRP laminates”, *Eng. Struct.*, **27**(5), 769-780.
- Baratta, A. and Corbi, I. (2012), “FRP composited retrofitting for protection of monumental and ancient constructions”, *Open Constr. Build. Technol. J.*, **6**, 361-367.
- Baratta, A., Corbi, I., Corbi, O., Barros, R.C. and Bairrão, R. (2012), “Shaking table experimental researches aimed at the protection of structures subject to dynamic loading”, *Open Constr. Build. Technol. J.*, **6**, 355-360.
- Calvi, G.M. (2013), “Choices and criteria for seismic strengthening”, *J. Earthq. Eng.*, **17**(6), 769-802.
- Christopoulos, C. and Filiatrault, A. (2006), *Principles of passive supplemental damping and seismic isolation*, IUSS Press, Istituto Universitario di Studi Superiori di Pavia, Italy.
- CNR-DT 200 (2004), *Guide for the design and construction of externally bonded FRP systems for strengthening existing structures*, National Research Council, Advisory Committee on technical recommendations for construction.
- Di Ludovico, M., Prota, A., Manfredi, G. and Cosenza, E. (2008), “Seismic strengthening of an under-designed rc structure with FRP”, *Earthq. Eng. Eng. Vib.*, **37**, 141-162.
- Eurocode 8 (2004), *Design of Structures for Earthquake Resistance - Part 3: Assessment and retrofitting of buildings*, C.E.N., European Committee for Standardization.
- FEMA 356, Federal Emergency Management Agency (2000), *Prestandard and commentary for the seismic rehabilitation of buildings*, American Society of Civil Engineers, Reston, Virginia.
- Ferracuti, B., Savoia, M., Pinho, R. and Francia, R. (2006), “Pushover analyses of FRP retrofitted RC frames”, *First ECEES*, Geneva, Switzerland.
- Filippou, F.C., Popov, E.P. and Bertero, V.V. (1983), “Modelling of R/C joints under cyclic excitations”, *J. Struct. Eng.*, **109**(11), 2666-2684.
- Gasparini, D. and Vanmarcke, E. (1976), “Simulated earthquake motions compatible with prescribed

- response spectra”, Massachusetts Institute of Technology, Department of Civil Engineering, USA.
- Iervolino, I., Maddaloni, G. and Cosenza, E. (2008), “Eurocode 8 compliant record sets for seismic analysis of structures”, *J. Earthq. Eng.*, **12**(1), 54-90.
- Mainstone, R.J. (1974), “Supplementary note on the stiffness and strength of infilled frames”, *Current Paper CP13/74, Building Research Establishment*, London.
- Mander, J.B., Priestley, M.J.N. and Park, R. (1988), “Theoretical stress–strain model for confined concrete”, *J. Struct. Eng.*, ASCE, **114**(8), 1804-1826.
- Martinez-Rueda, J.E. and Elnashai, A.S. (1997), “Confined concrete model under cyclic load”, *Mater. Struct.*, **30**(197), 139-147.
- Mazza, F. (2014), “Modeling and nonlinear static analysis of reinforced concrete framed buildings irregular in plan”, *Eng. Struct.*, **80**, 98-108.
- Mazza, F. and Vulcano, A. (2007), “Control of the along-wind response of steel framed buildings by using viscoelastic or friction dampers”, *Wind Struct.*, **10**(3), 233-247.
- Mazza, F. and Vulcano, A. (2008a), “Displacement-based seismic design procedure for framed buildings with dissipative braces. Part I: Theoretical formulation”, *In 2008 Seismic Engineering International Conference commemorating the 1908 Messina and Reggio Calabria Earthquake (MERCEA08)*, Reggio Calabria (Italy), American Institute of Physics Conference Proceedings, USA.
- Mazza, F. and Vulcano, A. (2008b), “Displacement-based seismic design procedure for framed buildings with dissipative braces. Part II: Numerical results”, *In 2008 Seismic Engineering International Conference commemorating the 1908 Messina and Reggio Calabria Earthquake (MERCEA08)*, Reggio Calabria (Italy), American Institute of Physics Conference Proceedings, USA.
- Mazza, F. and Vulcano A. (2011), “Sistemi di controllo passivo delle vibrazioni. Progettazione sismo-resistente di edifici in cemento armato”, *Città Studi Edizioni, Novara (Italy)*, **11**, 525-575. (in Italian)
- Mazza, F. and Vulcano, A. (2012), “Effects of near-fault ground motions on the nonlinear dynamic response of base-isolated RC framed buildings”, *Earthq. Eng. Struct. Dyn.*, **41**(2), 211-232.
- Mazza, F. and Vulcano, A. (2013), “Nonlinear seismic analysis to evaluate the effectiveness of damped braces”, *Int. J. Mech.*, **7**(3), 251-261.
- Mazza, F. and Vulcano, A. (2014a), “Design of hysteretic damped braces to improve the seismic performance of steel and RC framed structures”, *Int. J. Earthq. Eng.*, **31**(1), 1-12.
- Mazza, F. and Vulcano, A. (2014b), “Equivalent viscous damping for displacement-based seismic design of hysteretic damped braces for retrofitting framed buildings”, *Bull. Earthq. Eng.*, **12**(6), 2797-2819.
- Mazza, F., Vulcano, A. and Mazza, M. (2012), “Nonlinear dynamic response of rc buildings with different base-isolation systems subjected to horizontal and vertical components of near-fault ground motions”, *Open Constr. Build. Technol. J.*, **6**, 373-383.
- Menegotto, M. and Pinto, P.E. (1973), “Method of analysis for cyclically loaded reinforced concrete plane frames including changes in geometry and nonelastic behavior of elements under combined normal force and bending”, *In IABSE Symposium on Resistance and Ultimate Deformability of Structures Acted on by Well Defined Repeated Loads*, Lisbon.
- Monti, G. and Nuti, C. (1992), “Nonlinear cyclic behaviour of reinforcing bars including buckling”, *J. Struct. Eng.*, **118**(12), 3268-3284.
- Mpampatsikos, V., Nascimbene, R. and Petrini, L. (2008), “A critical review of the RC frame existing building assessment procedure according to Eurocode 8 and Italian seismic code”, *J. Earthq. Eng.*, **12**(S1), 52-82.
- Naeim, F. and Kelly, J.M. (1999), *Design of seismic isolated structures: from theory to practice*, John Wiley & Sons Ltd., New York, USA.
- Oliveto, G. and Marletta, M. (2005), “Seismic retrofitting of reinforced concrete buildings using traditional and innovative techniques”, *ISET J. Earthq. Technol.*, **42**(2-3), 21-46.
- Ponzo, F.C., Di Cesare, A., Nigro, D., Vulcano, A., Mazza, F., Dolce, M. and Moroni, C. (2012), “JET-PACS project: dynamic experimental tests and numerical results obtained for a steel frame equipped with hysteretic damped chevron braces”, *J. Earthq. Eng.*, **16**(5), 662-685.
- Romão, X., Delgado, R. and Costa, A. (2010), “Practical aspects of demand and capacity evaluation of RC

- members in the context of EC8-3”, *Earthq. Eng. Struct. Dyn.*, **39**(5), 473-499.
- Royal Decree-Law No. 640 (1935), *New text of the Technical Building Regulations, with special prescriptions for localities affected by earthquakes 1935*. (in Italian)
- Royal Decree-Law No. 2105 (1937), *Technical Building Regulations, with special prescriptions for localities affected by earthquakes*. (in Italian)
- Royal Decree-Law No. 2229 (1939), *Regulations for the construction of not reinforced and reinforced buildings 1939*. (in Italian)
- SeismoStruct (2010), *A computer program for static and dynamic nonlinear analysis of framed structures*, available from URL: <http://www.seismosoft.com>.
- Sorace, S. and Terenzi, G. (2008), “Seismic protection of frame structures by fluid viscous damped braces”, *J. Struct. Eng.*, ASCE, **134**(1), 45-55.
- NTC08 (2008), *Technical Regulations for the Constructions*, Italian Ministry of the Infrastructures. (in Italian)
- Thermou, G.E. and Elnashai, A.S. (2006), “Seismic retrofit schemes for rc structures and local-global consequences”, *Prog. Struct. Eng. Mater.*, **8**(1), 1-15.
- Tirca, L.D., Foti, D. and Diaferio, M. (2003), “Response of middle-rise steel frames with and without passive dampers to near-field ground motions”, *Eng. Struct.*, **25**(2), 69-179.

SA